Corneal-Reflection-Based Wide Range Gaze Tracking for a Car

Nagamatsu, Takashi

Hiroe, Mamoru

Rigoll, Gerhard

Corneal-Reflection-based Wide Range Gaze Tracking for a Car

Takashi Nagamatsu[1], Mamoru Hiroe[1], and Gerhard Rigoll[2]

[1] Kobe University, 5-1-1 Fukae-minami, Higashi-nada, Kobe, Japan
nagamatu@kobe-u.ac.jp,173w107w@stu.kobe-u.ac.jp
[2] Technical University of Munich, Germany
rigoll@tum.de

Abstract. When an eye tracking system is used in a car, user-calibration-free system is suitable because a driver can sometimes change. In addition, we usually look at the mirrors while driving a car, and so the system should track the driver's gaze in a wide range. In this study, we proposed a new method that calculates the gaze directions in a wide range by improving a user-calibration-free gaze tracking method. Our new method changes the calculation method based on the detected number of feature points of the eye. We installed cameras and LEDs in a car simulator that used a real car in a laboratory based on a simulator for developing a gaze sensitive environment. The evaluation results of a developed system for one participant showed that the system could track gazes when the participant looked mirrors.

Keywords: Gaze tracking, Car, Corneal reflection, Calibration free

1 Introduction

Most of accurate gaze tracking systems use a corneal-reflection-based method [1]. The system flushes the infrared light to the user and the system calculates the gaze from the relation between the corneal reflection and the pupil center.

Gaze tracking systems are beneficial for the safety of a car. For example, by checking the gaze of a driver, the system can alert the driver when the driver is not looking at the pedestrian who is crossing the road. If such an accident were to unfortunately occur, the driver's behavior while driving can be checked; it is useful to investigate the cause of the accident.

The corneal reflection-based gaze trackers are often used for gaze tracking in a car [2, 3]. Many gaze tracking systems can measure the gaze as long as the driver is looking straight ahead. However, it is difficult to measure peripheral gaze directions. One way to achieve wide range gaze tracking is adding cameras [4]. It raises the cost of a gaze tracking system.

On the other hand, in the case where an eye tracking system is used in a car, a user-calibration-free system is suitable because a driver can sometimes change.

In this paper, we describe a wide range gaze tracking system that encompasses a calibration-free function. Our work is similar to the Model's work [5],

which only shows the case in computer displays. Our approach is more flexible than theirs because of the application of the simulator for developing gaze sensitive environment proposed by Nagamatsu et al. [6].

The contributions of our work are as follows:

- to propose a new calculation method for corneal-reflection based gaze tracking system when some of the feature points of the eye images are not detected.
- to show the feasibility of the gaze calculation method for mirror-looking scenario for a car.

2 Related works

The method of the reconstruction of the optical axis of the eye differs depending on the system configuration (i.e. number of cameras and light sources). General theory of remote gaze estimation is described in detail in Gustrin's work [7]. On the basis of their work, if at least two cameras and two light sources are used, the reconstruction of the optical axis of the eye can be achieved without a user-specific calibration procedure. If one camera and multiple light sources are used, the reconstruction of the optical axis of the eye can be achieved when some of the user-specific parameters (i.e., radius of the cornea R, distant between centers of the cornea and pupil K) are known. If one camera and one light source are used, the reconstruction of the optical axis of the eye can be achieved when the distance between the camera and the eye is known in addition to R and K. Therefore, the system with two cameras and two light sources are suitable from the aspect of the user calibration procedure and user's head movement.

On the other hand, the measurable range of a system using two cameras is smaller than that of a system using one camera. Model et al. proposed a method to extend a tracking range of two-camera system by switching two-camera system to one-camera systems after determine the user-specific parameters [5].

Nagamatsu et al. proposed the mathematical model to calculate the gaze measurable range [8]. The range is represented as overlapping area of cones that is called *gaze cone*. The gaze cone is formed by the relation between eye, camera, and light source. Based on the gaze cone, they proposed a simulator for developing gaze sensitive environment [6].

3 User-calibration free gaze tracking method

This section describes an existing method of calibration-free gaze estimation, which helps to understand our proposed method. Here, bold faces indicate 3D vector.

3.1 Eye model

Figure 1 shows a typical model of an eye that is used in the model-based approach [9, 7, 10, 11]. The model contains a mixture of large and small spheres. The cornea

is modeled as a small sphere. There are two important axes: one is the optical axis, which is the line passing through the geometric center of the eye, and the other is the visual axis, which is the line of sight connecting the fovea and the point of gaze (POG). It is approximated that the two axes of the eye intersect at the center of the corneal curvature. The difference between the optical and visual axes is called angle κ.

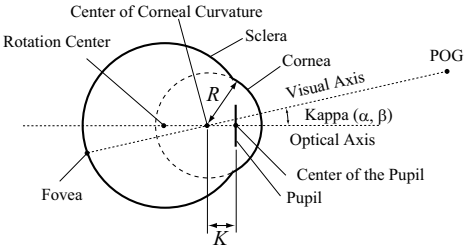

Fig. 1. Eye model

There are five user-specific parameters (R,K, α, β, and n_2), where R is the radius of the corneal curvature, K is the distance between the centers of the cornea and the pupil, α is the horizontal component of the angle κ, β is the vertical component of the angle κ, and n_2 is the effective refractive index of the cornea; in this paper, we assume n_2 is constant.

3.2 Estimation of the position of the corneal center[12]

Figure 2 shows a ray tracing diagram for the estimation of the optical axis of the eye. $\mathbf{L}_i$ is the position of the light source i ($i = 0, 1$) and $\mathbf{O}_j$ is the nodal point of camera j ($j = 0, 1$). The value of $\mathbf{L}_i$ is measured and $\mathbf{O}_j$ is determined by the camera calibration beforehand. A ray from $\mathbf{L}_i$ is reflected on the corneal surface such that it passes through $\mathbf{O}_j$ and intersects the camera image plane at a point $\mathbf{G}'_{ji}$ (glint: reflection on the outer surface of the cornea). The plane including $\mathbf{O}_j$, $\mathbf{L}_i$, and $\mathbf{G}'_{ji}$ is expressed as

$$\{(\mathbf{G}'_{ji} - \mathbf{O}_j) \times (\mathbf{L}_i - \mathbf{O}_j)\} \cdot (\mathbf{X} - \mathbf{O}_j) = 0, \tag{1}$$

where $\mathbf{X} = (x, y, z)^{\mathrm{T}}$ is a point on the plane. When a ray is reflected on a spherical corneal surface, the plane passing through the incident and reflection vectors includes the center of the sphere $\mathbf{C}$; i.e. the plane expressed by Equation 1 includes $\mathbf{C}$. There exist four planes represented by the Equation 1. $\mathbf{C}$ is determined by the intersection of these planes.

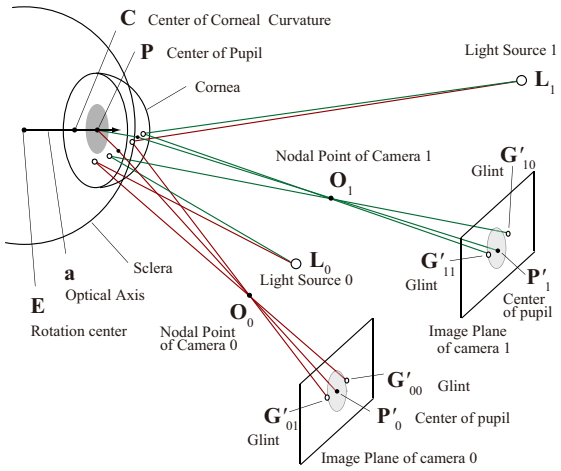

Fig. 2. Ray tracing diagram

3.3 Estimation of the optical axis of the eye

The optical axis $\mathbf{a}$ is obtained by the equation as follows:

$$\mathbf{a} = \frac{((\mathbf{O}_0 - \mathbf{P}'_0) \times (\mathbf{C} - \mathbf{O}_0)) \times ((\mathbf{O}_1 - \mathbf{P}'_1) \times (\mathbf{C} - \mathbf{O}_1))}{||((\mathbf{O}_0 - \mathbf{P}'_0) \times (\mathbf{C} - \mathbf{O}_0)) \times ((\mathbf{O}_1 - \mathbf{P}'_1) \times (\mathbf{C} - \mathbf{O}_1))||}, \tag{2}$$

where $\mathbf{P}'_0$ and $\mathbf{P}'_1$ are the pupil center positions on the image sensor of camera 0 and 1, respectively.

3.4 Estimation of the visual axis of the eye

There are several approaches to estimate the angle κ [13, 14]. In this stage of this study, we adopted the method by Nagamatsu et al. [13], which estimates the angle κ by averaging both of the optical axes of the eyes. After the angle κ is obtained, we can calculate the visual axis of the eye when the eye rotates.

4 Applying to a car simulator

4.1 Simulation for developing a gaze-sensitive environment in a car

We used a simulator for developing a gaze sensitive environment for a car proposed by Nagamatsu et al. [6]. The simulator is based on the mathematical model proposed by Nagamatsu et al. [8], which is a common model for corneal reflection-based gaze trackers. According to the model, the measuring range of gaze direction forms a cone, which is called gaze cone (Figure 3).

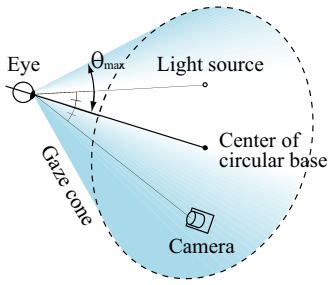

Fig. 3. Gaze cone; the range of the gaze direction in which the light reflected on corneal surface

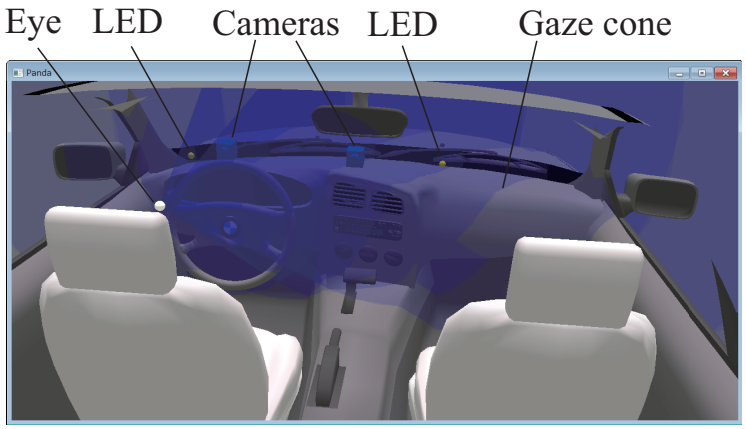

Fig. 4. Simulator for developing a gaze-sensitive environment in a car

Figure 4 shows the screen image of the simulator. In Figure 4, four gaze cones for the right eye (transparent blue), two cameras (blue), and two LEDs (yellow) are shown. We can move the positions of the cameras, eyes, and LEDs.

We used a calibration-free gaze tracking method described in Section 3. The method requires the overlapping area of at least three gaze cones, so that the intersection of Equations 1 makes a point.

By using this simulator, we adjusted the position of the cameras and LEDs, so that three gaze cones have overlapping areas in the front direction and at least one gaze cone contains each side mirror. Figure 5 shows the simulation result.

4.2 Installing gaze tracker in a car simulator

After deciding the positions of cameras and LEDs, we installed them in a car simulator (Figure 6) as shown in Figure 7 . This system consisted of two monochrome GigE digital cameras (HXG20NIR, Baumer GmbH), projector, and a laptop

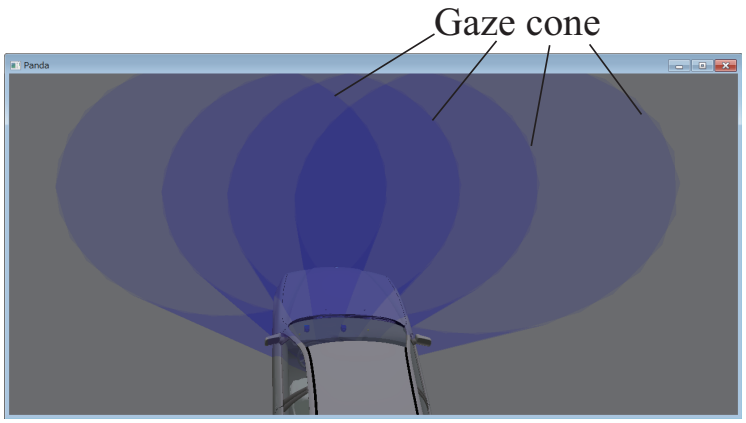

Fig. 5. Simulation result

Windows-based PC (Windows 7). Each camera was equipped with a 2/3" CMOS image sensor with a resolution of 2048 × 1088 pixels. A 16-mm lens and a visible light cut filter were attached to each camera. These cameras were positioned under the display. IR-LEDs were attached to the rear view mirror and left pillar of the car, and the positions were measured. The camera parameters were determined beforehand. The software was developed using OpenCV in C++ language. The diameter of the pupil in the captured image was approximately 30 pixels.

Fig. 6. Car simulator in laboratory

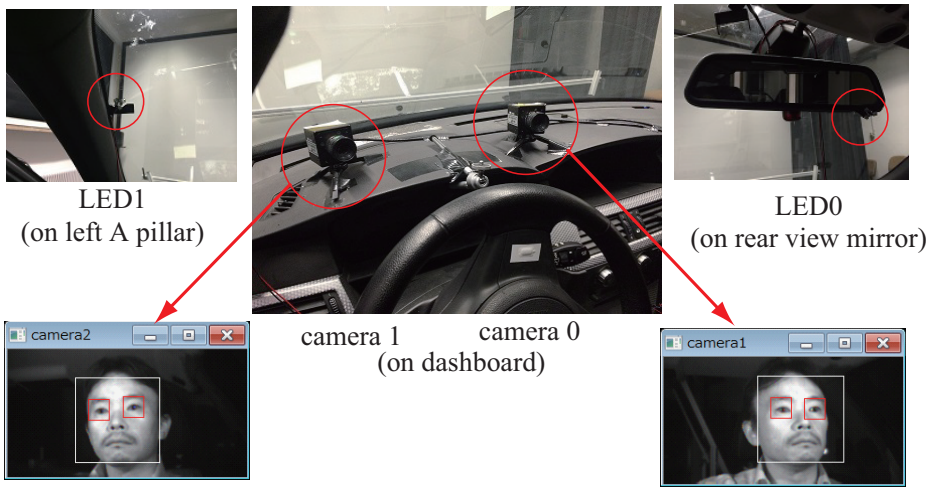

Fig. 7. Installation of cameras and LEDs

4.3 CG software for displaying gazes

The point of gaze can be displayed on the front screen by the projector. However, the gazes for when the driver looked at the mirrors were not shown on the screen because the screen size was not wide enough. Therefore, we developed CG software that displays the gaze as shown in Figure 8. The visual axes of the right and left eyes are expressed in green and red, respectively.

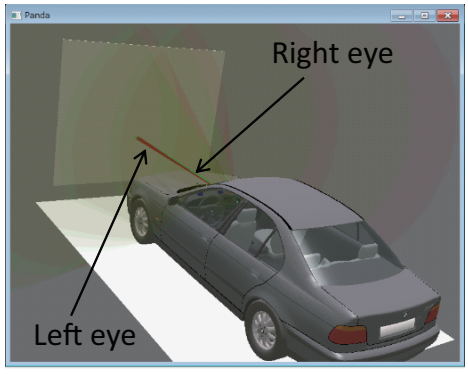

Fig. 8. CG software for displaying gazes

5 New gaze calculation method to achieve wide range gaze tracking

5.1 Problem when eye rotates largely

When a driver looked forward in the car simulator, the gaze tracking system based on the method described in Section 3 detected the feature points of the eye (glints and pupil centers) as shown in Figure 9, and estimated the visual axes of both the eyes as shown in Figure 8. However, when the eyes rotate largely, e.g. the user looked at the mirrors, the system could not estimate the visual axis of the eye.

When the user rotates the eye more than a certain limit, some of the light from the LEDs become not to reflect on the cornea as shown in Figure 10; it was predicted by the simulation.

Therefore, in order to measure the wide range of gaze (i.e. various positions and directions of the eye), we propose a calculation method when some of the feature points are not detected.

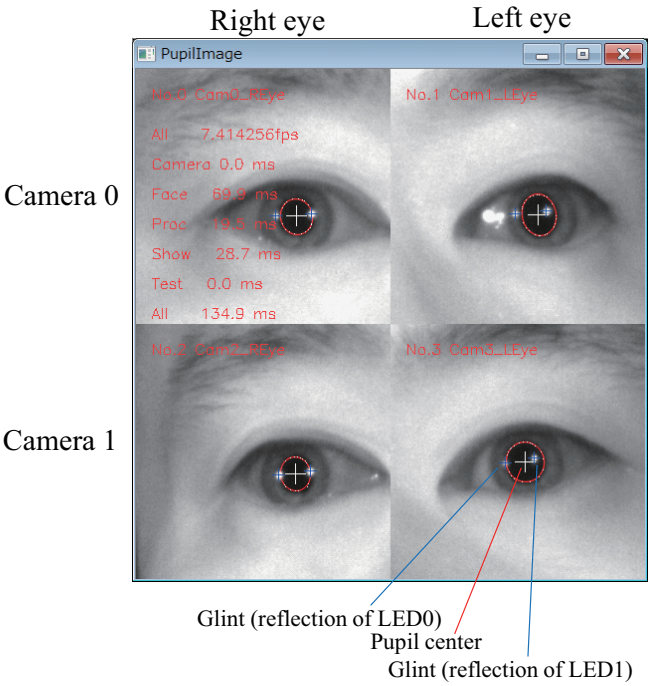

Fig. 9. Detected feature point when the driver looks forward

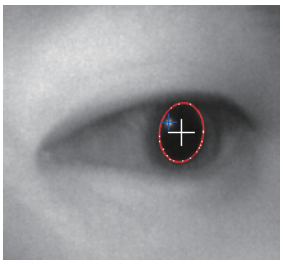

Fig. 10. Eye image when the eye rotate largely. Only one of two glints is detected.

5.2 Classification of cases of detected feature points

We considered calculation methods when some of the glints are not detected or one of the pupils is not detected. We divided the situations into three cases. Figure 11 shows cases according to the detected feature points. These cases were classified by the number of detected glints (cyan) and pupil center (red). It is to be noted that 0 and 1 (regarding the camera number) can be replaced.

The following sections describes calculation methods for each case.

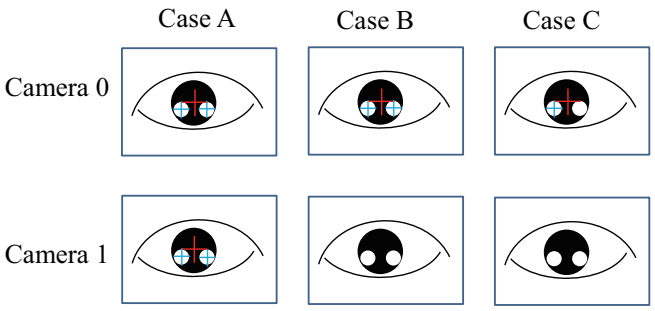

Fig. 11. Cases according to the detected points

5.3 Calculation method for case A

In this case, all feature points are detected and the optical axis is calculated based on the existing method described in Section 3. We estimate that most of driving falls under this case because the driver looks forward most of the time.

In addition to the optical axis, here, we calculate R, K, the vector between glints, and the angle κ, which are used for the calculation of other cases.

Calculating R Figure 12 shows a plane that includes, $\mathbf{L}_i$, $\mathbf{O}_j$, and $\mathbf{C}$. The estimation procedure of R is as follows.

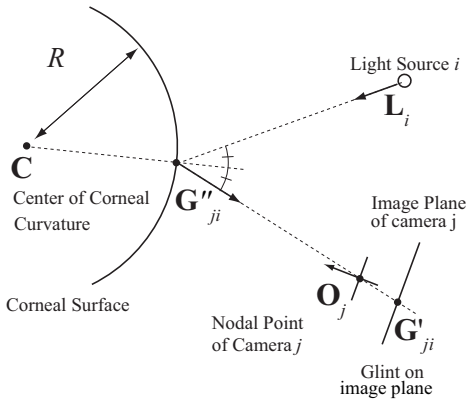

Fig. 12. Plane of reflection.

After setting the initial R, $\mathbf{G}''_{ji}$ is calculated by the intersection of the corneal sphere ($R = ||\mathbf{X} - \mathbf{C}||$) and the line ($\mathbf{X} = \mathbf{O}_j + t(\mathbf{O}_j - \mathbf{G}'_{ji})$). Then, the normal vector of the corneal sphere at $\mathbf{G}''_{ji}$ ($\mathbf{G}''_{ji} - \mathbf{C}$), the incident vector ($\mathbf{G}''_{ji} - \mathbf{L}_i$), and the reflection vectors ($\mathbf{O}_j - \mathbf{G}''_{ji}$) are calculated. Then, R is determined so that the incident angle is equal to the reflection angle. R can be found between about 6-9 mm (the average of the radius of the cornea is about 7.8 mm).

Calculating K Figure 13 shows a plane that contains $\mathbf{C}$, $\mathbf{P}$ (pupil center), and $\mathbf{O}_j$.

As R is determined by the above method, $\mathbf{P}''_j$ is calculated by the intersection of the corneal sphere ($R = ||\mathbf{X} - \mathbf{C}||$) and the line ($\mathbf{X} = \mathbf{O}_j + t(\mathbf{O}_j - \mathbf{P}'_j)$). The refracted vector at $\mathbf{P}''_j$ ($\mathbf{t}_j$) is calculated using Snell's law as,

$$\mathbf{t}_j = \left(-\rho \mathbf{n}_j \cdot \mathbf{v}_j - \sqrt{1 - \rho^2 \left(1 - (\mathbf{n}_j \cdot \mathbf{v}_j)^2\right)} \right) \mathbf{n}_j + \rho \mathbf{v}_j, \tag{3}$$

where $\rho = n_1/n_2$, n_1 is the refractive index of the air (≈ 1), n_2 is the effective refractive index of the cornea (≈ 1.3375), $\mathbf{v}_j = (\mathbf{O}_j - \mathbf{P}'_j)/||\mathbf{O}_j - \mathbf{P}'_j||$ is the incident vector at $\mathbf{P}''_j$, and $\mathbf{n}_j = (\mathbf{P}''_j - \mathbf{C})/||\mathbf{P}''_j - \mathbf{C}||$is the unit normal vector at $\mathbf{P}''_j$.

The center of the pupil $\mathbf{P}$ is calculated by the intersection between the two lines $\mathbf{X} = \mathbf{P}''_0 + t\mathbf{t}_0$ and $\mathbf{X} = \mathbf{P}''_1 + s\mathbf{t}_1$, where t,s are parameters. Thus, K is calculated as $K = ||\mathbf{P} - \mathbf{C}||$

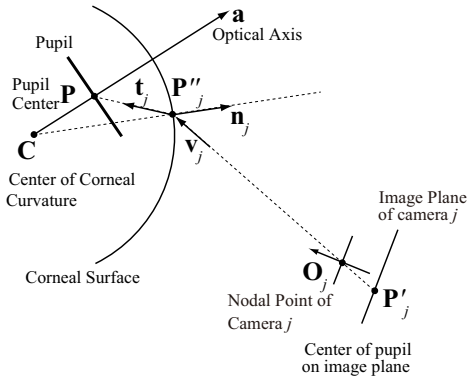

Fig. 13. Plane including the optical axis

Calculating the vector between glints The vector between glints is saved in case A, which is used for the calculation of case C.

Calculating angle κ (α, β) When the results of detection of the feature points of both the eyes are classified to the case A, we calculate the angle κ (α, β) by Nagamatsu's method [13]. α and β are used in case B or case C to calculate the optical axis of the eye.

5.4 Calculation method for case B

In this case, two glints and a pupil center are detected using camera 0, and no glint and no pupil center are detected using camera 1. This situation may happen when the driver looks at mirrors. The following method is effective after R and K are estimated.

The center of the corneal curvature should be on the intersection line made by the two planes: $((\mathbf{G}'_{00} - \mathbf{O}_0) \times (\mathbf{L}_0 - \mathbf{O}_0)) \cdot (\mathbf{X} - \mathbf{O}_0) = 0$ and $((\mathbf{G}'_{01} - \mathbf{O}_0) \times (\mathbf{L}_1 - \mathbf{O}_0)) \cdot (\mathbf{X} - \mathbf{O}_0) = 0$. The unit direction vector of the intersection line is as follows.

$$\mathbf{l} = \frac{((\mathbf{G}'_{00} - \mathbf{O}_0) \times (\mathbf{L}_0 - \mathbf{O}_0)) \times ((\mathbf{G}'_{01} - \mathbf{O}_0) \times (\mathbf{L}_1 - \mathbf{O}_0))}{||((\mathbf{G}'_{00} - \mathbf{O}_0) \times (\mathbf{L}_0 - \mathbf{O}_0)) \times ((\mathbf{G}'_{01} - \mathbf{O}_0) \times (\mathbf{L}_1 - \mathbf{O}_0))||}, \tag{4}$$

Then, $\mathbf{C}$ is expressed using $\mathbf{l}$ as $\mathbf{C} = \mathbf{O}_0 + u\mathbf{l}$, where u is a parameter. u is calculated as follows.

When the initial value of u is set, $\mathbf{C}$ is calculated. $\mathbf{G}''_{0i}$ is calculated by the intersection of the corneal sphere ($R = ||\mathbf{X} - \mathbf{C}||$) and the line ($\mathbf{X} = \mathbf{O}_0 + t(\mathbf{O}_0 - \mathbf{G}''_{0i})$). Then, u is determined so that the incident angle is equal to the reflection angle at $\mathbf{G}''_{0i}$. Since u is a distance between the camera and the eye, it can be found between about 300-900 mm. Thus, we can estimate the position of the center of the corneal curvature $\mathbf{C}$.

The corneal sphere is determined by $R = ||\mathbf{X} - \mathbf{C}||$. The refraction vector $\mathbf{t}_0$ is described as Equation 3. Therefore, the position of the pupil center $\mathbf{P}$ is expressed as $\mathbf{X} = \mathbf{P}'_0 + v\mathbf{t}_0$. v is determined to satisfy $K = ||\mathbf{P} - \mathbf{C}||$. v is smaller than the radius of the cornea. It is enough to search v in the range of 0 – 9 mm.

5.5 Calculation method for case C

In this case, one glint and a pupil center are detected using camera 0, and no glint and no pupil center are detected using camera 1. When the eyeball rotates greater than a certain limit, the light cannot reflect on the cornea. The number of reflections on the cornea decreases to one.

In a car, the driver is sitting, so the driver's movement is limited. Therefore, we estimates that the distance between the camera and the eye is almost constant.

We add a virtual glint on the eye image using the vector between glints saved in case A, so that the relative position between the two glints are the same as that when the driver looks forward.

Then, we can use the calculation method in case B.

6 Evaluation

6.1 Method

For evaluation, we made a scenario as shown in Figure 14. In this scenario, the driver looked in the order as follows.

1. The driver looked forward.
2. The driver looked at the rear view mirror intending to move only his eyes.
3. The driver looked at the rear view mirror naturally.
4. The driver looked forward.
5. The driver looked at the right mirror intending to move only his eyes.
6. The driver looked at the right mirror naturally.
7. The driver looked forward.
8. The driver looked at the left mirror intending to move only his eyes.
9. The driver looked at the left mirror naturally.

The reason why the driver looked at the front and the mirrors alternately was that the calculations of cases B and C need to be calculated after case A (the driver sees the front).

We captured images of camera 0 and 1 when a driver looking at four directions: forward, the rear view mirror, the right mirror, and the left mirror. For each direction, two sets of images of camera 0 and 1 were saved. Using saved eight sets of images, we calculated gazes and thier accuracies.

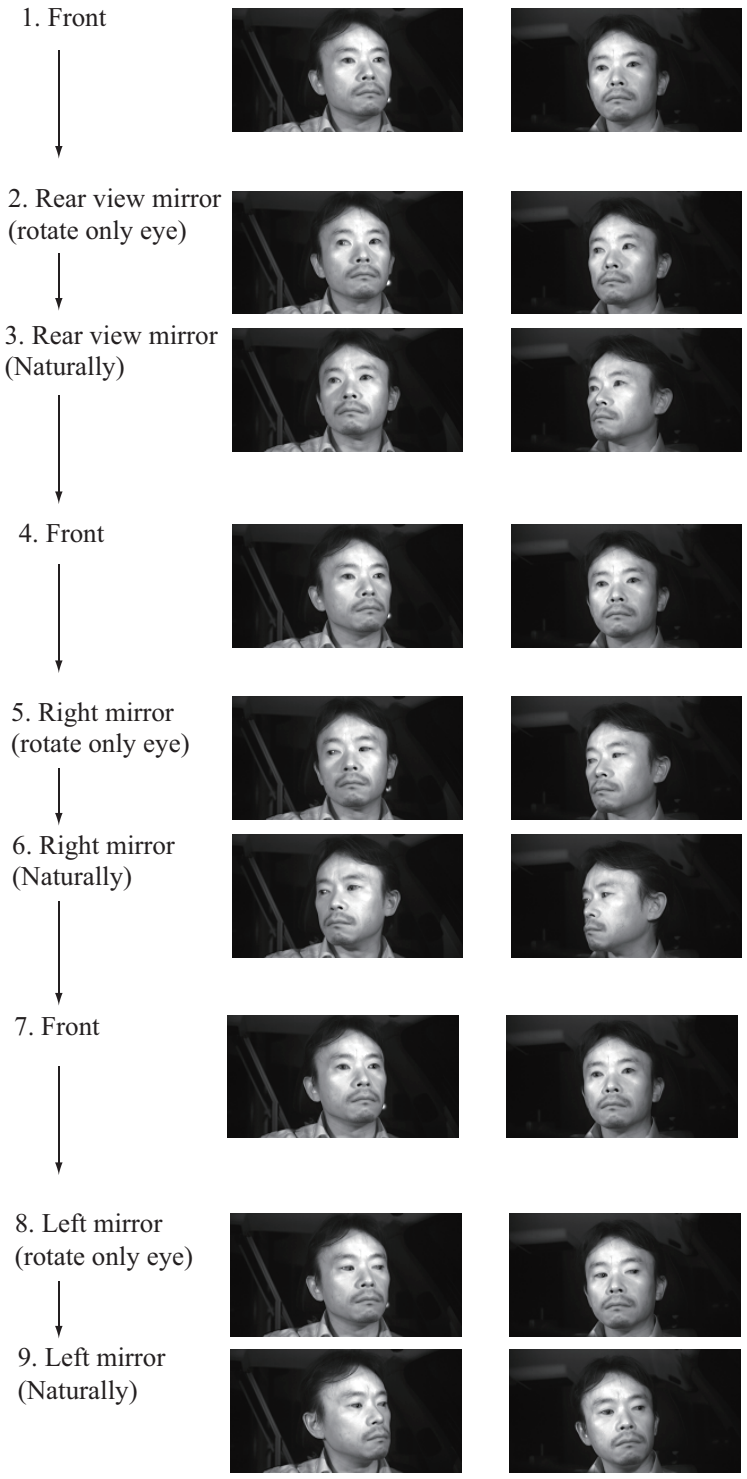

Fig. 14. Scenario

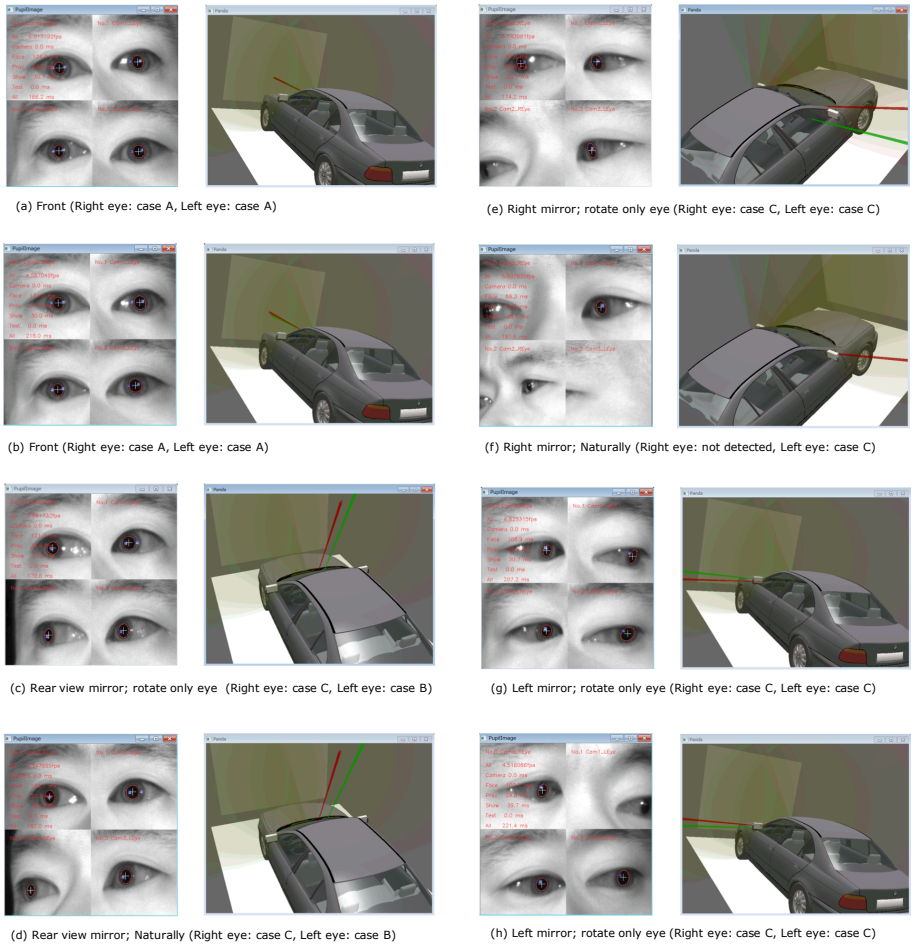

Fig. 15. Eye images and visual axes of both eyes in CG

6.2 Results

Figure 15 shows the eye images and the visual axes of both eyes in CG based on the scenario.

Figure 15 (a) and (b) show the case where the driver looked forward. In this case, all the feature points were detected, so the calculation is conducted by the calculation method in case A. Figure 15 (c) and (d) show the cases where the driver looked at the rear view mirror. The visual axes of the right and left eyes were calculated by the methods in case C and case B, respectively. Figure 15 (e) shows the case where the driver looked at the right mirror rotating only his eyes . The visual axes of the right and left eyes were calculated by the method in

case C. Figure 15 (f) shows the case where the driver looked at the right mirror naturally. The visual axis of the right eye were not detected, and the visual axes of the left eye were calculated by the method in case C. Figure 15 (g) and (h) show the cases where the driver looked at the left mirror. The visual axes of the right and left eyes were calculated by the methods in case C. Thus, the system could track gazes when the driver looked mirrors.

Table 1 shows the accuracy in degree when the driver looked at the mirrors. The first row shows the mirror that the driver looked at. The second row shows left (L) or right (R) eye. The third row is the results when the driver looked at the mirrors intending to rotate only his eyes. The fourth row is the results when the driver looked at the mirrors naturally.

Table 1. Accuracy (degree).

Mirror	Rear-view		Right		Left	
Eye	L	R	L	R	L	R
looked intending to rotate only his eyes	14.9	3.4	7.4	13.0	7.4	1.7
looked naturally	14.3	1.2	7.1	-	0.4	3.4

6.3 Discussion

We proposed a novel method to achieve wide range gaze tracking, and evaluated it for one participant; it worked well. However, evaluation of this method is insufficient, so we will increase the number of participants.

Although we applied the proposed method described in Section 5 to a car simulator, this method can be generally applied to all the situations when the corneal reflection is partially not detected. For example, the situations happen when the resolution of the camera is low, when the eyeball rotates largely, when the hand blocks the camera or the light source, or when the user blinks.

7 Conclusion

We proposed a novel calculation method of a gaze tracker for a car when the driver rotates their eyes largely. At that time, some of the feature points of the eye images are not detected. Our proposed method changes the calculation method based on the detected feature points of the eye. We implemented the method and installed it in a car simulator in a laboratory. The evaluation results for one participant showed that the system could track gazes when the participant looked mirrors. The accuracy was 0.4–14.9 degrees.

Acknowledgement

This work was supported by JSPS KAKENHI Grant Numbers 23300047, 16H02860.
.

References

1. Hansen, D.W., Ji, Q.: In the eye of the beholder: A survey of models for eyes and gaze. IEEE Transactions on Pattern Analysis and Machine Intelligence **32**(3) (2010) 478–500
2. Trosterer, S., Meschtscherjakov, A., Wilfinger, D., Tscheligi, M.: Eye tracking in the car: Challenges in a dual-task scenario on a test track. In: Adjunct Proceedings of the 6th International Conference on Automotive User Interfaces and Interactive Vehicular Applications, ACM (2014) 1–6
3. Fletcher, L., Zelinsky, A.: Driver inattention detection based on eye gaze-road event correlation. The international journal of robotics research **28**(6) (2009) 774–801
4. SmartEye. http://smarteye.se/research-instruments/se-pro/
5. Model, D., Eizenman, M.: A general framework for extension of a tracking range of user-calibration-free remote eye-gaze tracking systems. In: Proceedings of the Symposium on Eye Tracking Research and Applications, ACM (2012) 253–256
6. Nagamatsu, T., Yamamoto, M., Rigoll, G.: Simulator for developing gaze sensitive environment using corneal reflection-based remote gaze tracker. In: Proceedings of the 2nd ACM symposium on Spatial user interaction, ACM (2014) 142–142
7. Guestrin, E.D., Eizenman, M.: General theory of remote gaze estimation using the pupil center and corneal reflections. IEEE Transactions on Biomedical Engineering **53**(6) (2006) 1124–1133
8. Nagamatsu, T., Yamamoto, M., Sugano, R., Kamahara, J.: Mathematical model for wide range gaze tracking system based on corneal reflections and pupil using stereo cameras. In: Proceedings of the Symposium on Eye Tracking Research and Applications, ACM (2012) 257–260
9. Shih, S.W., Liu, J.: A novel approach to 3-d gaze tracking using stereo cameras. IEEE Transactions on Systems, Man, and Cybernetics, Part B **34**(1) (2004) 234–245
10. Nagamatsu, T., Kamahara, J., Iko, T., Tanaka, N.: One-point calibration gaze tracking based on eyeball kinematics using stereo cameras. In: Proceedings of the 2008 Symposium on Eye Tracking Research & Applications. (2008) 95–98
11. Villanueva, A., Cabeza, R.: A novel gaze estimation system with one calibration point. IEEE Transactions on Systems, Man, and Cybernetics, Part B **38**(4) (2008) 1123 – 1138
12. Nagamatsu, T., Kamahara, J., Tanaka, N.: Calibration-free gaze tracking using a binocular 3d eye model. In: Proceedings of the 27th international conference extended abstracts on Human factors in computing systems, ACM (2009) 3613–3618
13. Nagamatsu, T., Sugano, R., Iwamoto, Y., Kamahara, J., Tanaka, N.: User-calibration-free gaze estimation method using a binocular 3d eye model. IEICE Transactions on Information and Systems **E94-D**(9) (2011) 1817–1829
14. Model, D., Eizenman, M.: User-calibration-free remote gaze estimation system. In: Proceedings of the 2010 Symposium on Eye-Tracking Research & Applications, ACM (2010) 29–36